Volume 7 | Number 42 | 14 November 2015 | Pages 17575–17982

Nanoscale

www.rsc.org/nanoscale

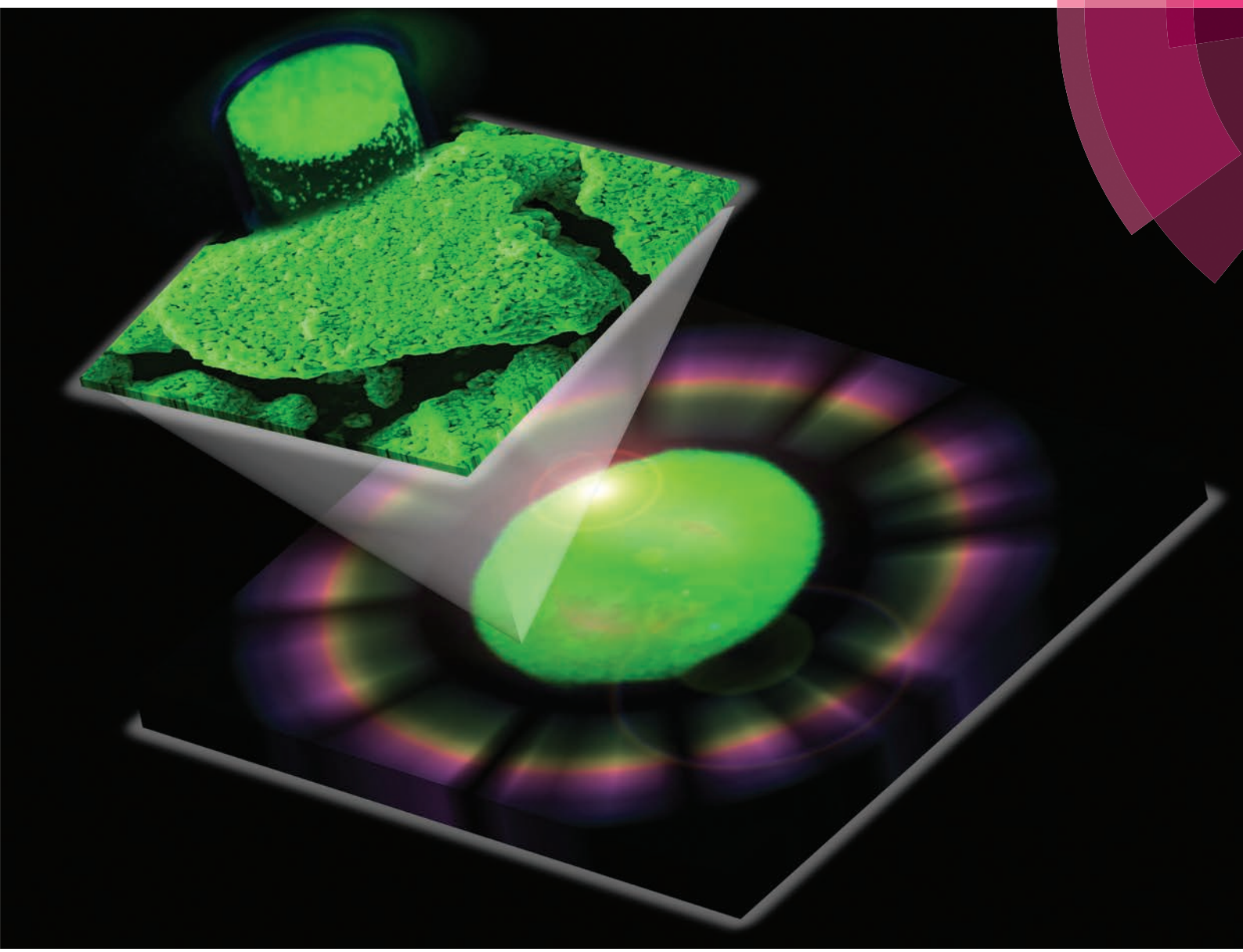

ISSN 2040-3364

ROYAL SOCIETY OF CHEMISTRY

COMMUNICATION

Hilmi Volkan Demir *et al.*

Stable and efficient colour enrichment powders of nonpolar nanocrystals in LiCl

NCNST

Nanoscale

COMMUNICATION

View Article Online
View Journal | View Issue

Cite this: *Nanoscale*, 2015, **7**, 17611

Received 26th April 2015,
Accepted 22nd July 2015

DOI: 10.1039/c5nr02696b

www.rsc.org/nanoscale

Stable and efficient colour enrichment powders of nonpolar nanocrystals in LiCl†

Talha Erdem,‡[a] Zeliha Soran-Erdem,‡[a] Vijay Kumar Sharma,[b] Yusuf Kelestemur,[a] Marcus Adam,[c] Nikolai Gaponik[c] and Hilmi Volkan Demir*[a,b]

In this work, we propose and develop the inorganic salt encapsulation of semiconductor nanocrystal (NC) dispersion in a nonpolar phase to make a highly stable and highly efficient colour converting powder for colour enrichment in light-emitting diode backlighting. Here the wrapping of the as-synthesized green-emitting CdSe/CdZnSeS/ZnS nanocrystals into a salt matrix without ligand exchange is uniquely enabled by using a LiCl ionic host dissolved in tetrahydrofuran (THF), which simultaneously disperses these nonpolar nanocrystals. We studied the emission stability of the solid films prepared using NCs with and without LiCl encapsulation on blue LEDs driven at high current levels. The encapsulated NC powder in epoxy preserved 95.5% of the initial emission intensity and stabilized at this level while the emission intensity of NCs without salt encapsulation continuously decreased to 34.7% of its initial value after 96 h of operation. In addition, we investigated the effect of ionic salt encapsulation on the quantum efficiency of nonpolar NCs and found the quantum efficiency of the NCs-in-LiCl to be 75.1% while that of the NCs in dispersion was 73.0% and that in a film without LiCl encapsulation was 67.9%. We believe that such ionic salt encapsulated powders of nonpolar NCs presented here will find ubiquitous use for colour enrichment in display backlighting.

1. Introduction

Within the last thirty years following their first report,[1] colloidal nanocrystals (NCs) have witnessed a tremendous improvement in their synthesis, crystal quality, and quantum efficiency.[2] As a consequence of these developments, today NCs are being extensively used in various applications from biology[3] to optoelectronics including light-emitting diodes (LEDs)[4–6] and lasers.[7,8] In particular, the tunability of the NC emission and its narrow bandwidth have attracted significant attention for their use in display backlighting[9] and general lighting[4,5] as colour converters on light-emitting diodes.

Despite their improved quantum efficiencies, the NCs still remain vulnerable to the solid film preparation process using polymer based encapsulants since the quantum efficiencies of the NCs significantly decrease in the polymer film. In addition, due to the continuous exposure to energetic photons and elevated temperatures, the emission intensity of the NCs decreases undesirably on light-emitting diodes (LEDs). In particular, the use of these LEDs for long durations causes significant degradation of NC emission. To improve the emission stability of the NCs, silica coating was proposed; however, this eventually adversely affects the quantum efficiency of the NCs.[10] As an alternative, Otto *et al.* demonstrated for the first time that aqueous NCs can be incorporated into a single phase process in salt crystals (*e.g.*, NaCl, KCl, *etc.*) and this improves the emission stability of the NCs.[11] Another study reported by Müller *et al.* showed that these salt crystals also improve the quantum efficiency of the aqueous NCs.[12] Subsequently, we applied this single-phase approach to plasmonic systems and demonstrated plasmonic fluorescence enhancement of the aqueous NCs this time together with the aqueous metal nanoparticles co-immobilized in sucrose host crystals.[13] In all the previous reports,[11–14] however, only aqueous NCs (or other aqueous nanoparticles) could be used. In the case of using aqueous NCs, the as-synthesized NCs in water are plagued with intrinsically low quantum efficiencies. Alternatively, high-efficiency nonpolar NCs could be used only after ligand exchange, which also suffered from substantially reduced quantum efficiencies upon the ligand exchange. Therefore, in either case, the quantum efficiency of the resulting ionic salt encapsulated aqueous NCs in a single phase has been a problem. However, the utilization of nonpolar NCs is significantly important because of their high efficiencies and narrow

[a]*Departments of Electrical and Electronics Engineering, Physics, UNAM – National Nanotechnology Research Center, and Institute of Materials Science and Nanotechnology, Bilkent University, 06800, Turkey. E-mail: volkan@bilkent.edu.tr, hvdemir@ntu.edu.sg*

[b]*School of Electrical and Electronic Engineering and School of Physical and Mathematical Sciences, Nanyang Technological University, 639798, Singapore*

[c]*Physical Chemistry, TU Dresden, Bergstrasse 66b, D-01062 Dresden, Germany*

†Electronic supplementary information (ESI) available. See DOI: 10.1039/c5nr02696b

‡These authors contributed equally to this paper.

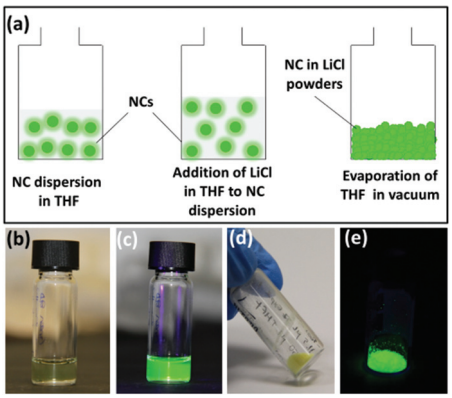

Fig. 1 (a) Schematics of NC encapsulation into LiCl salt. The real colour images of NC dispersion in THF (b) under ambient lighting and (c) UV illumination at 366 nm. The real colour images of the NCs-in-LiCl powders (d) under ambient lighting and (e) UV illumination at 366 nm.

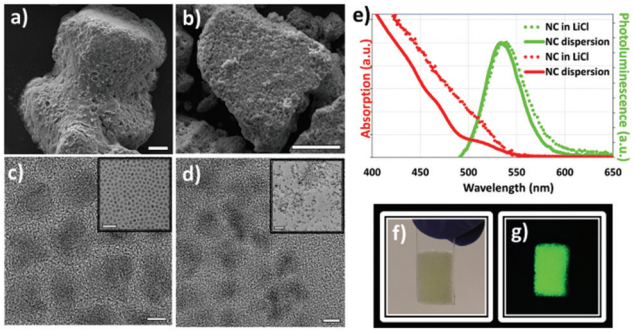

Fig. 2 Scanning electron microscopy (SEM) images of the LiCl powders (a) without and (b) with NCs (scale bars: 30 μm). Transmission electron microscopy (TEM) images of (c) the as-synthesized NC dispersion in hexane and (d) the NC-in-LiCl powders (scale bars of larger images: 5 nm and inset images: 50 nm). (e) Photoluminescence spectra of the nonpolar NCs in dispersion and the same NCs encapsulated within LiCl ionic salt. Also, absorption spectra of the as-synthesized NCs (dispersion in hexane) and NC-in-LiCl powder film were provided. Real colour photographs of the LiCl encapsulated NC film under (f) ambient lighting and (g) UV illumination at 366 nm.

emission bandwidths. Acquiring a narrow emission is very essential for the displays and general lighting applications while high quantum efficiencies in particular in the blue and green colours are needed to address the green gap problem of the epitaxial LEDs.[4,5]

As a solution, here we propose and demonstrate incorporation of the nonpolar NCs directly into the LiCl ionic salt without ligand exchange by benefiting from the solubility of LiCl in tetrahydrofuran (THF), which simultaneously disperses these nonpolar NCs. As a proof-of-concept demonstration, we integrated green-emitting CdSe/CdZnSeS/ZnS NCs into the LiCl host (Fig. 1) and characterized their structural and optical properties. In addition, we tested their emission stability on a blue LED operating at 100 mA for 96 h. At the end of the test, the NCs encapsulated into LiCl succeeded in preserving 95.5% of their initial emission intensity while that of the NCs without LiCl encapsulation decreased to 34.7%. To uncover the effect of the LiCl encapsulation on the emission capabilities of the NCs, we measured reproducibly the quantum efficiency of the NCs-in-LiCl host to be 75.1% which is higher than the quantum efficiency of the same as-synthesized nonpolar NCs in dispersion (73.1%) and the same ones in the film without salt encapsulation (67.9%). Subsequently, we investigated the emission dynamics of the NCs-in-LiCl and observed that their radiative decay lifetime is consistent with the theoretical predictions relating the radiative lifetime to the variation of the dielectric environment. Considering all these, we believe that the proposed LiCl encapsulation of the nonpolar NCs will find wide-scale use in light-emitting devices as colour enrichment films of display backlights.

2. Results and discussion

We integrated nonpolar NCs-in-LiCl powders as described in the Experimental section and Fig. 1. Briefly, we mixed the oversaturated LiCl solution (in THF) with NCs dispersed in THF in a nitrogen environment. Subsequently, the solvent was evaporated under vacuum and consequently NC encapsulated powders were obtained. The NC weight percentage in these powders was determined to be ~1.22%. Further structural characterizations were performed using scanning electron microscopy (SEM) and transmission electron microscopy (TEM) (Fig. 2).

The SEM images of the representative LiCl powders with and without NC loading show that the size of the powders is in general less than 200 μm for both the cases with and without NC loading and they do not exhibit crystal facets as opposed to slower crystallizations previously studied in other media.[13] This is mainly due to the fast evaporation of the solvent (THF in this case) under vacuum. Another interesting feature is the occurrence of small grape-like structures on the powders containing NCs while such an observation cannot be made for the LiCl powders without NC loading (Fig. S2(a) and (b)†). Here it is worth noting that the NCs are small and cannot be imaged using SEM. Each of these grape-like structures most likely includes many NCs inside. We think that these grape-like structures may possibly play a role in preventing full aggregation of the NCs within LiCl and thus avoid quenching of the NCs.

Furthermore, we used TEM to image the NCs without LiCl and the NCs incorporated into LiCl (Fig. 2(c) and (d)). These images show that the size of our as-synthesized NCs is approximately 8 nm. In addition, we imaged the NC-in-LiCl powder (Fig. 2(d) and S3†) and observed that the NCs in LiCl tend to be localized in some parts of the salt. Finally, having the information of size and concentration of our NCs, we are able to estimate the molar concentration of the NCs inside the LiCl host (see the ESI† for the details). Our calculation reveals that there are between 13.0 and 18.4 pmol of NCs inside 1 mg of powder.

Following the morphological characterization, we prepared the NC-in-LiCl film as explained in the Experimental method section using a commercial epoxy that does not require any UV or heat treatment for hardening. Subsequently, we measured the steady-state photoluminescence spectra and quantum efficiencies of the NCs in the dispersion and encapsulated into the LiCl host. We observed that the encapsulation of the NCs by the ionic salt causes a slight red shift in the emission spectrum (Fig. 2(e)) as observed in previous studies,[11,12] which can be explained by the limited aggregation of the NCs within LiCl (Fig. 2(d) and S3†) and also in part by the interactions of dipoles of the NCs with the dipoles of the surrounding medium as also reported by Ibnaouf *et al.*[15] The quantum efficiency of the NCs-in-LiCl was measured to be 75.1% while the quantum efficiency of the same NCs in dispersion was found to be 73.0% and that of the NCs without LiCl encapsulation in the solid film remained at 67.9%. The observation of this increased quantum efficiency of the nonpolar NCs in the salt matrix agrees well with the previous reports of salt encapsulation of aqueous NCs in NaCl.[12,14]

Here, we also analysed the emission kinetics of the NCs in dispersion and the same NCs encapsulated by the LiCl salt. The measured time-resolved photoluminescence spectra presented in Fig. 3 revealed a lifetime of 29.1 ns for the NCs dispersed in hexane and 19.4 ns for the NCs encapsulated in LiCl. Using the quantum efficiency (η) information together with the lifetime (τ_{total}), the effective radiative lifetime (τ_{rad}) is predicted using eqn (1).

$$\eta = \frac{1/\tau_{rad}}{1/\tau_{total}} \quad (1)$$

This analysis leads to a radiative lifetime of 39.9 ns for the NCs dispersed in hexane while that of the NCs-in-LiCl decreases to 25.8 ns. This decrease of the radiative decay time can be mainly attributed to the variation of the dielectric medium from hexane in the case of the NC dispersion to LiCl in the case of the NC salt encapsulation. To test this hypothesis, we first calculated the radiative lifetime of the NCs in vacuum using the measured values in the dispersion by employing the virtual cavity, empty cavity, and fully-microscopic models[16] (see the ESI† for details). Subsequently, we predicted the radiative lifetimes of the NCs using this value when they are surrounded by the LiCl matrix and presented the results in Table 1 in the rows indicated by the names of these models. The computed results show that the predicted experimental and theoretical radiative lifetimes are reasonably close especially when the empty cavity model is considered. Therefore, we can conclude that the dipoles generated in the NCs encapsulated by the LiCl salt experience a radiative recombination that is not significantly affected by the local field of the surrounding medium generating the cavity.

Table 1 The quantum efficiency of the NCs in dispersion and the same NCs encapsulated in LiCl; their total lifetimes and radiative recombination lifetimes. In addition, the radiative lifetimes of the NCs in vacuum were first calculated by employing the radiative lifetime of the NCs in dispersion, then these values were used to predict the radiative lifetime of the NCs in the LiCl matrix according to the empty cavity, virtual cavity, and fully microscopic models

	Quantum efficiency (%)	τ_{total} (ns)	τ_{rad} (ns)
NCs in dispersion	73.0	29.1	39.9
NCs-in-LiCl	75.1	19.4	25.8
Empty cavity model	—	—	28.7
Virtual cavity model	—	—	21.9
Fully microscopic model	—	—	32.5

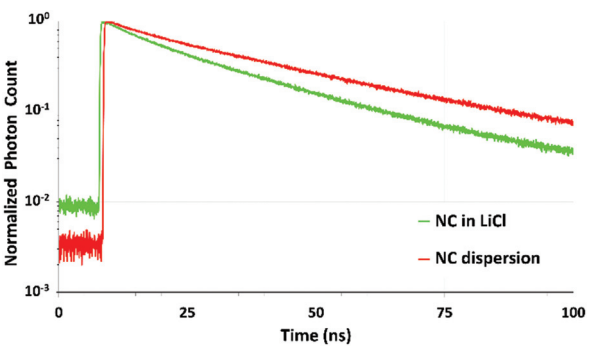

Fig. 3 Time-resolved photoluminescence decay curves of the NCs in dispersion and the same NCs encapsulated in LiCl.

In addition to the effect of the surrounding dielectric medium on the quantum efficiency, we also expect the ionic salts wrapping the NCs to improve the stability of the NC emission on LEDs. For this purpose, we tested the emission stability of the NC-in-LiCl powders blended with epoxy on a blue LED driven at a high current level (Fig. 4(a) and (b)) while the NCs without LiCl encapsulation blended with epoxy was our control group. We observed that the efficiency of the NCs without LiCl encapsulation decreased to 34.7% of its initial value after 96 h (four days) of uninterrupted operation while the film of NC-in-LiCl powders successfully preserved 95.5% of its initial quantum efficiency during the same period. In terms of the absolute quantum efficiencies, the quantum efficiency of the NC-in-LiCl powders decreased from 75.1% to 71.7% while that of the NCs without LiCl encapsulation dropped from 67.9% to below 23.6% at the end of the test (Fig. 4c). We attribute this improvement in the emission stability of the NCs on a LED driven at high currents to the formation of a physical barrier against oxygen penetration by the LiCl salt limiting the interaction with the ambient environment. This improved stability is of significant importance especially for the display backlighting.

To test whether a chemical interaction occurs between the ligands of the NCs and the host medium during the crystallization process, we measured the FTIR spectrum of the NCs without LiCl encapsulation, the NCs-in-LiCl, and only LiCl salt (Fig. S4†). However, we could not see any indication of a potential chemical interaction. In order to gain further structural information, we performed thermal gravimetric analysis (TGA)

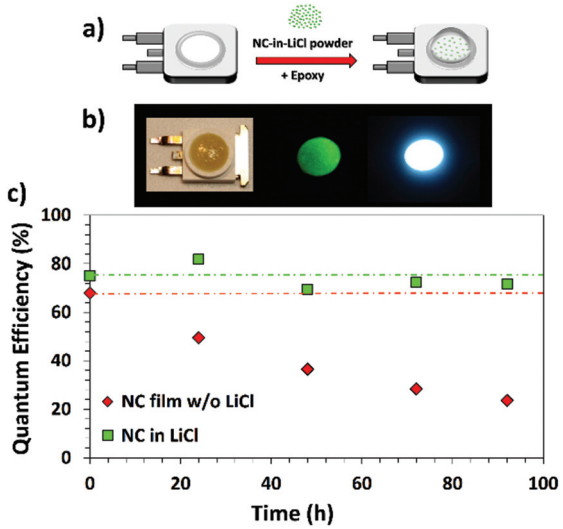

Fig. 4 (a) Schematic image of NC-in-LiCl film preparation onto LED for the temperature stability test. (b) Real colour images of the NCs-in-LiCl on a blue LED under ambient lighting, UV illumination at 366 nm, and when LED is driven, from left to right. (c) Quantum efficiency variation of the NCs with and without LiCl encapsulation as a function of time when they are integrated on the blue LED driven at a high current level for 96 h (four days).

on the samples of only NC, only LiCl, NC-in-LiCl powder and NC drop-casted LiCl powder (Fig. S5, and see the ESI† for further details). We observed rapid evaporation of LiCl beyond its melting point (~605 °C), and addition of NCs shifted this process toward lower temperatures. However, the characteristics of the weight loss curves of the NC-in-LiCl powders and NC drop-casted LiCl powders are very similar to each other, which inform us that this fastened evaporation is more likely a physical process rather than an indication of a chemical interaction. In addition, from the TGA curves we could not observe any signature that we can relate to any indication of the NC–salt chemical interaction. As a result, using TGA, we were not able to identify an obvious chemical interaction between the NCs and the host matrix. To further investigate the interaction of the LiCl with the NCs, we performed X-ray photoelectron spectroscopy (XPS) of only NCs, NC-in-LiCl powders, and only LiCl powders (see the ESI for further details, Fig. S6 and S7†). This analysis also did not provide any indication of a notable chemical interaction between the salt medium and the NCs.

3. Experimental

3.1 Chemicals

Cadmium oxide (CdO, 99.99%), zinc acetate ($Zn(acetate)_2$, 99.9%), sulfur (S, 99.9%), selenium (Se, 99.99%), potassium bromide (KBr) and lithium chloride (LiCl) were purchased from Sigma-Aldrich in powder form. Oleic acid (OA, 90%), trioctylphosphine (TOP, 90%), 1-octadecene (1-ODE, 90%), dodecanethiol (DDT, 99%), tetrahydrofuran (THF) and hexane were bought from Sigma-Aldrich and used without any purification.

3.2 NC synthesis

CdSe/CdZnSeS/ZnS nanocrystals were synthesized by following the method in the literature.[17] For a typical synthesis, 0.4 mmol of CdO, 4 mmol of $Zn(acetate)_2$, 5.6 mL of OA and 20 mL of 1-ODE were loaded into a 50 mL three-necked flask. After degassing for 2 h at 100 °C under vigorous stirring, the temperature of the mixture was increased to 310 °C under argon flow. At this temperature, 0.1 mmol of Se powder and 4 mmol of S powder both dissolved in 3 mL of TOP were quickly injected into the reaction flask. After 1 min, 0.3 mL of DDT dissolved in 0.8 mL of 1-ODE was injected dropwise and the temperature of the reaction flask was set to 300 °C. Following 10 min of growth, the mixture was cooled down to room temperature and precipitated with a hexane/acetone mixture. Finally, the resulting nanocrystals were dissolved in hexane and used for further experiments.

3.3 Preparation of the LiCl encapsulated NC powders

An oversaturated stock solution of LiCl was prepared by mixing 1.83 g of LiCl in 50 mL of THF in a glovebox with nitrogen environment. Prior to the encapsulation of the NCs-in-LiCl, hexane of the NC dispersion was evaporated. We optimized the NC amount to maximize their photoluminescence quantum efficiency in the salt (see Fig. S1†) and chose the sample with 0.4 mg of the NCs to use, which resulted in the highest quantum efficiency of 75.1%, throughout the rest of this work. Before the preparation of NC-in-LiCl powders, the NCs were first dispersed in 250 μL of THF, and then 1 mL of LiCl stock solution was slowly added to NCs in THF. Subsequently, the samples were placed within a desiccator to completely evaporate the solvent and to obtain the LiCl encapsulated NCs. NC weight percentages in the powders were determined by re-dissolving them in THF and comparing the NC absorbance values with the NC dispersion. The methodology for estimating the molar concentration of the NCs inside the powders is explained in the ESI.† Only LiCl powders were obtained using the same procedure without NC addition. The NC-in-LiCl films were prepared by mixing ~6.3 mg of the NC embedded LiCl powders with a commercial two-component epoxy (Bison), which does not require any UV or heat treatment for hardening. Since we aimed to test the stabilities of NC-in-LiCl powders on LEDs at a high current level, we chose this encapsulant on purpose. However, other encapsulants such as commercial silicones or poly(methyl methacrylate), which in general require heat treatment or UV exposure for hardening, can also be used with these powders.

3.4 Structural characterization

Detailed information on SEM, TEM, FTIR, TGA, and XPS is provided in the ESI.†

3.5 Steady-state and time-resolved fluorescence spectroscopy

Steady-state photoluminescence spectra of NC dispersion and the NC-in-LiCl film were recorded using a Spectral Products monochromator integrated xenon lamp as the excitation source, a Hamamatsu integrating sphere, and an Ocean Optics Maya 2000 spectrometer. Time-resolved fluorescence spectra were recorded using a PicoHarp 200 time-resolved single photon counting system (PicoQuant). A pulsed laser emitting at 375 nm was employed as the excitation source and the time difference between the time of the maximum photon count and the time 1/e of the maximum photon count was reported as the lifetime.

3.6 Quantum efficiency measurements

The quantum efficiency measurements were performed at an excitation wavelength of 460 nm using a Spectral Products monochromator integrated xenon lamp, a Hamamatsu integrating sphere, and an Ocean Optics Maya 2000 spectrometer using the following method, also previously described by de Mello *et al.*[18] This technique involves three steps: (i) the measurement of the spectrum when no sample is placed in the integrating sphere, (ii) the measurement of the spectrum when the sample is directly illuminated by the excitation source, and (iii) the measurement of the sample when the sample is not directly illuminated by the light source and instead illuminated by the light scattered from the surface of the integrating sphere. Here, in step (ii), the sample was placed with a slightly oblique angle as suggested. In step (iii), the sample was rotated so that only the scattered light excited the sample. In Fig. 5, an illustration of this technique is presented and the quantum efficiency (η) is calculated using eqn (2). In this equation, E stands for the excitation part of the spectrum while L stands for the emission part of the measured spectrum. The subscripts i, ii, and iii indicate the measurement steps described above.

$$\eta = \frac{L_{ii} - \frac{E_{ii}L_{iii}}{E_{iii}}}{\left(1 - \frac{E_{ii}}{E_{iii}}\right)E_i} \quad (2)$$

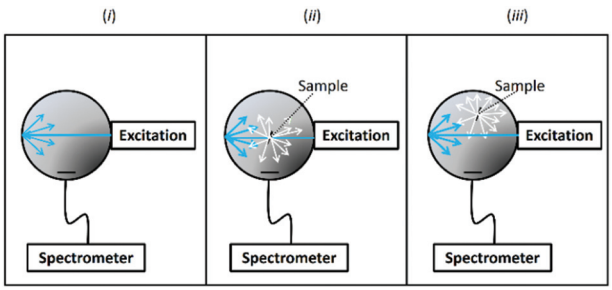

Fig. 5 Illustration of the quantum efficiency measurement methodology: (i) the measurement of the excitation spectrum without sample, (ii) the measurement of the spectrum when the sample is directly excited by the light source, and (iii) the measurement of the spectrum when the sample is excited by the light that scatters from the surface of the integrating sphere.

The accuracy of the measurement setup was tested using Rhodamine 6G dissolved in ethanol with an optical density <0.1 at 460 nm. We measured a quantum efficiency of 94.7%, which is in agreement with the standard value of 95%.

3.7 Emission stability tests

The emission stability of the films was tested by investigating the emission intensity of the NCs with and without LiCl encapsulation on an Avago ASMT blue LED driven at 100 mA for 96 h (four days). The NCs with LiCl encapsulation were coated on the LED chip using the two-component epoxy. As the control group, the NCs without LiCl were coated on the blue LED by first drop-casting the NCs on the LED and then the epoxy was added and blended with the NCs following the evaporation of the solvent.

4. Conclusions

In summary, we present here the encapsulation of the colloidal as-synthesized nanocrystals by the LiCl ionic salts in the form of a powder, which significantly improves the stability of the encapsulated NCs on LEDs operating at high currents. We also observed that the LiCl encapsulation helps in preserving the in-dispersion quantum efficiency levels of the NCs for use in the colour enrichment films. Additionally, unlike the previous reports on the incorporation of the aqueous NCs in salt or sucrose matrices, this method totally removes the need for a ligand exchange of the nonpolar NCs, which is known to otherwise suffer from decreased quantum efficiencies during the phase transfer. Considering all these strong aspects, we believe that the proposed encapsulation technique presented here will find wide-spread use in the light-emitting diodes of display backlights integrated with NCs as colour enrichment films.

Acknowledgements

We acknowledge ESF EURYI, EU-FP7 Nanophotonics4Energy NoE, BMBF TUR 09/001, and TUBITAK EEEAG 109E002, 109E004, 110E010, 110E217, 112E183 and the support in part by NRF-CRP-6-2010-02 and NRF-RF-2009-09. H. V. D. acknowledges additional support from TUBA-GEBIP and T. E. acknowledges support from TUBITAK BIDEB.

Notes and references

1 R. Rossetti, J. Ellison, J. Gibson and L. Brus, *J. Chem. Phys.*, 1984, **80**, 4464–4469.
2 *Nat. Nanotechnol.*, 2014, **9**, 325.
3 X. Michalet, F. F. Pinaud, L. A. Bentolila, J. M. Tsay, S. Doose, J. J. Li, G. Sundaresan, A. M. Wu, S. S. Gambhir and S. Weiss, *Science*, 2005, **307**, 538–544.
4 T. Erdem and H. V. Demir, *Nanophotonics*, 2013, **2**, 57–81.

5 H. V. Demir, S. Nizamoglu, T. Erdem, E. Mutlugun, N. Gaponik and A. Eychmüller, *Nano Today*, 2011, **6**, 632–647.
6 X. Yang, Y. Ma, E. Mutlugun, Y. Zhao, K. S. Leck, S. T. Tan, H. V. Demir, Q. Zhang, H. Du and X. W. Sun, *ACS Appl. Mater. Interfaces*, 2014, **6**, 495–499.
7 C. Dang, J. Lee, C. Breen, J. S. Steckel, S. Coe-Sullivan and A. Nurmikko, *Nat. Nanotechnol.*, 2012, **7**, 335–339.
8 B. Guzelturk, Y. Kelestemur, M. Z. Akgul, V. K. Sharma and H. V. Demir, *J. Phys. Chem. Lett.*, 2014, **5**, 2214–2218.
9 E. Jang, S. Jun, H. Jang, J. Lim, B. Kim and Y. Kim, *Adv. Mater.*, 2010, **22**, 3076–3080.
10 S. Jun, J. Lee and E. Jang, *ACS Nano*, 2013, **7**, 1472–1477.
11 T. Otto, M. Müller, P. Mundra, V. Lesnyak, H. V. Demir, N. Gaponik and A. Eychmüller, *Nano Lett.*, 2012, **12**, 5348–5354.
12 M. Müller, M. Kaiser, G. M. Stachowski, U. Resch-Genger, N. Gaponik and A. Eychmüller, *Chem. Mater.*, 2014, **26**, 3231–3237.
13 T. Erdem, Z. Soran-Erdem, P. L. Hernandez-Martinez, V. K. Sharma, H. Akcali, I. Akcali, N. Gaponik, A. Eychmüller and H. V. Demir, *Nano Res.*, 2015, **8**, 860–869.
14 Z. Soran-Erdem, T. Erdem, P. L. Hernandez-Martinez, M. Z. Akgul, N. Gaponik and H. V. Demir, *J. Phys. Chem. Lett.*, 2015, **6**, 1767–1772.
15 K. H. Ibnaouf, S. Prasad, M. S. Al Salhi, A. Hamdan, M. B. Zaman and L. El Emir, *J. Lumin.*, 2014, **149**, 369–373.
16 S. F. Wuister, C. de Mello Donega and A. Meijerink, *J. Chem. Phys.*, 2004, **121**, 4310–4315.
17 W. K. Bae, K. Char, H. Hur and S. Lee, *Chem. Mater.*, 2008, **20**, 531–539.
18 J. C. de Mello, H. F. Wittmann and R. H. Friend, *Adv. Mater.*, 1997, **9**, 230–232.